

Coupled Membrane Transporters Reduce Noise

Luca Cardelli and Luca Laurenti
University of Oxford

Attila Csikasz-Nagy
King's College London & Pázmány Péter Catholic University

Molecular systems are inherently probabilistic and operate in a noisy environment, yet, despite all these uncertainties, molecular functions are surprisingly reliable and robust. The principles used by natural systems to deal with noise are still not well understood, especially in a non-homogeneous environment where molecules can diffuse across different compartments. In this paper we show that membrane transport mechanisms have very effective properties of noise reduction. In particular, we show that active transport mechanisms (those requiring energy and that can transport against a gradient of concentration) such as symporters and antiporters, have surprising efficiency in noise reduction, which outperforms passive diffusion mechanism and are well below Poisson levels. We link our results to the coupled transport of potassium, sodium and glucose to show that the noise in internal glucose level can be greatly reduced. Our results show that compartmentalization can be a highly effective mechanism of noise reduction and suggests that membrane transport could give this extra benefit, contributing to the emergence of complex compartmentalization in eukaryotes.

INTRODUCTION

Molecular processes contain an inherent element of stochasticity due to reactions involving molecules present in low numbers. Such a noise interferes with cellular functions and propagates to all dependent processes [8]. For example, noise in mRNA transcription propagates to translation processes often leading to super-Poisson variability in protein levels [6]. Hence, at a first sight, it seems impossible that complex multi-step processes may exhibit highly controlled behaviour. Nevertheless, biological systems perform their functions in a surprisingly reliable way. Therefore, they must incorporate mechanisms that increase robustness and reduce noise [10].

In order to understand how natural systems can reduce the noise, molecular filters have been studied [11]. Molecular filters are *chemical reaction networks* that are able to reduce the noise of an input molecular signal. Examples of molecular filters include feedback and feed-forward loops [2], low-pass filters [13], and annihilation filters [11]. Many theoretical studies of these systems have been performed and lower bounds on their noise reduction capabilities have been derived [7, 11, 12]. However, the vast majority of the published works focus on noise reduction mechanisms in a homogeneous environment and at the single cell level, whereas much less is known about the effect that spatial compartmentalization can have on noise [17].

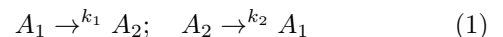
In this paper, we show that membrane transport mechanisms can act as efficient noise filters. In particular, we show that active transport mechanisms (those requiring energy and can transport against a gradient) outperform passive mechanisms of transport (facilitated diffusion in the direction of the gradient) in terms of noise reduction. The observed noise reduction does not require introduction of time delays, commonly used in other noise reducing mechanisms. In particular, we study how molecular

pumps that transport two molecule types in the same direction (symporters) or the opposite directions (antiporters) can reduce internal noise in cells well below Poisson levels. Furthermore, we use the derived results to investigate how sodium-potassium pumps in combination with sodium-glucose cotransporters can filter out external molecular noise and reduce the fluctuations in intracellular glucose levels.

The idea that compartmentalization can act as a noise filter is not new [17]. However, a deep mathematical analysis is lacking and all the theoretical results are mostly limited to passive diffusive transport mechanisms [15, 16]. Hence, our results provide a key step towards the understanding of the robustness properties of natural systems and, due to ubiquitous presence of cellular compartments in eukaryotic cells, suggest that spatial compartmentalization may be the predominant mechanism of noise reduction in eukaryotes.

UNIPORTER

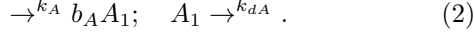
We start our analysis by considering a simple transport mechanism between two compartments (Figure 1.I.)



where molecules of species A are transported between two compartments and with A_i representing the number of molecules of species A in compartment i . This mechanism can correspond to facilitated diffusion if the transport follows the gradient of molecules across a permeable membrane ($k_1 = k_2$), but is often used also as a simplified model of other forms of membrane transport, such as the transport of *mRNA* from nucleus to cytoplasm [15].

We assume molecules of A appear in compartment 1 through extra-cellular transport according to a noise process, which includes bursts of dimension $b_A > 0$ and that

can be modelled by the following reactions



That is, A_1 appears in compartment 1 through a noisy process characterized by the following mean and Fano Factor (ratio between variance and expectation) at steady state

$$E[A_1]_\infty = \frac{b_A k_A}{k_{dA}} \quad F_{A_1} = \frac{1 + b_A}{2}. \quad (3)$$

For $b_A = 1$ we have Poisson noise (Fano Factor equals 1), while for $b_A > 1$ we have super Poisson noise.

Under this input process for A_1 , we can derive the exact expressions for expectation and Fano Factor of A_2 at steady state and we obtain

$$E[A_2]_\infty = \frac{b_A^2 k_A k_1}{k_{dA} k_2} \quad F_{A_2} = 1 + \frac{k_1 (b_A - 1)}{2(k_1 + k_2 + k_{dA})}. \quad (4)$$

The transport mechanism in Eqn (1) can filter noise when the transport is slow (k_1 small), but can never bring it below Poisson levels (Fano is lower bounded by 1). This confirms experimental observations in [1], where it is shown that slow nuclear export of transcripts may result in a reduced variability of transcripts without affecting mean abundance. Note however that this transport mechanism may be beneficial even when the transport is fast. In fact, when $k = k_1 = k_2$ we obtain $\lim_{k \rightarrow \infty} F_{A_2} = \frac{3+b_A}{4}$, which for $b_A > 1$ is always smaller than F_{A_1} . Note also that for the limit case $b_A = 1$ (Poisson noise) we see that $F_{A_2} = 1$ independently of the reaction rates.

Nevertheless, although the described mechanism can reduce noise, Eqn 4 implies that the noise reduction is inherently lower bounded by Poisson noise (Fano Factor of 1). In the following sections we show that coupled transport mechanisms allow one to obtain better noise reduction performances, and we link them to well studied symporters and antiporters [9].

SYMPORTER AND ANTIPORTER

The first coupled active transport we consider is a *symporter* (Figure 1.II.), inspired by transmembrane symporters. Membrane symporters are integral membrane proteins that are involved in the co-transport of different types of molecules across the cell membrane [9].

The symporter simultaneously transports molecules of species A and B from compartment 1 to compartment 2 and can be modelled with the following reactions



where A_i, B_i are molecules of species A and B in compartments $i \in \{1, 2\}$. The above mechanism is widely used to transport one of the molecules against concentration gradients while the other follows its gradient [9].

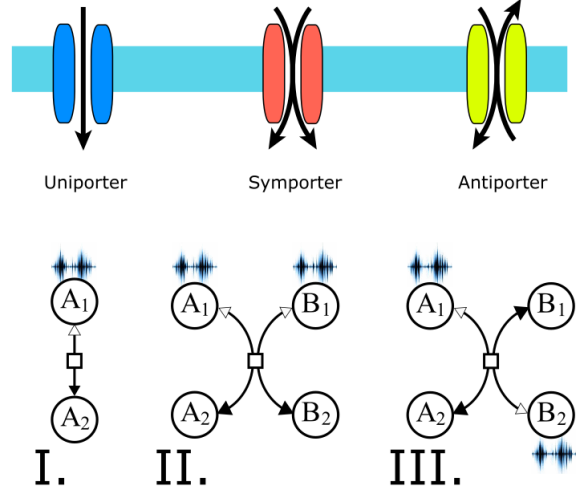


FIG. 1. Transporters: common trans-membrane transporters (top) and their respective reaction schemes (I.,II.,III.), where circles denote species and squares denote reversible reactions. Subscripts indicate compartment numbers (inside or outside the membrane). Direct reactions have solid arrowhead, while inverse (assumed weaker) reactions have hollow arrowheads. Ambient noise (indicated by noisy graphs) is applied to the input species.

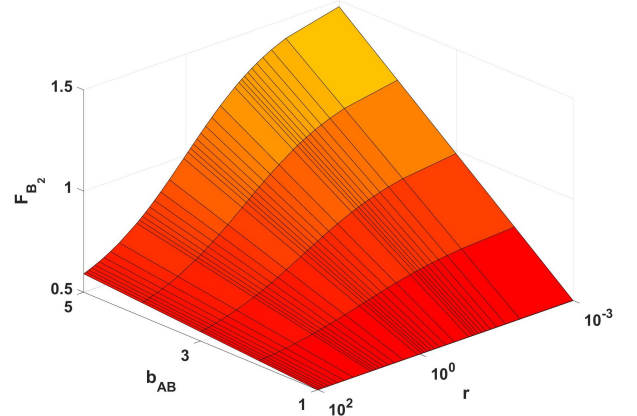
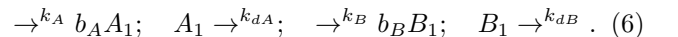


FIG. 2. Plot of upper bound of Fano factor of B_2 and A_2 at steady state as a function of the flux r and of b_{AB} . Lower bound is identically 0.5

In what follows, we show that this mechanism has also surprising properties for noise reduction. In order to illustrate this point, as for the previous case, we assume that A_1 and B_1 are subject to burst noise modelled as



We assume that in compartment 2 initially A and B are not present, but they are transported over time from compartment 1. Moreover, in order to obtain simple analytic expressions we assume $k_{dA} = k_{dB}$, and $b_A = b_B = b_{AB} \in \mathbb{N}$. That is A_1 and B_1 appear in compartment 1 according to similarly noisy processes with

average values respectively of $\frac{b_{AB}k_A}{k_{dA}}$ and $\frac{b_{AB}k_B}{k_{dB}}$. Furthermore, we consider that the parameter r controls the preferred direction and efficiency of the transporter, that is $k_2 = k_1 r$ for $r \in \mathbb{R}_{>0}$. Under these assumptions analytic expressions for F_{A_2} and F_{B_2} can be derived and it is possible to show that F_{A_2} and F_{B_2} monotonically increase with k_1 and are bounded between the following limits, which are obtained by varying k_1 between 0 and infinity (as detailed in Supplementary Material the bounds are obtained by solving the Lyapunov equation associated to the linear noise approximation of the Chemical Master Equation [19]).

$$\frac{1}{2} \leq F_{A_2} \leq \frac{k_A + b_{AB}k_A + 4\sqrt{k_A k_B r} + k_B + b_{AB}k_B}{4(k_A + 2\sqrt{k_A k_B r} + k_B)}. \quad (7)$$

and similarly for F_{B_2} .

Eqn (7) implies that for $b_{AB} = 1$ (Poisson noise), we always have

$$F_{A_2} = F_{B_2} = \frac{1}{2},$$

independently of the various parameters, while for $b_{AB} = 2$, we have F_{A_2} and F_{B_2} bounded between $\frac{1}{2}$ and $\frac{3}{4}$, still significantly below Poisson levels.

As the Fano factor of A_2 and B_2 is monotonic in k_1 , from Eqn (7) we also obtain that when k_1 is small enough, then the Fano factor of A_2 and B_2 will converge to $\frac{1}{2}$ independently of the various parameters. However, if k_1 is not small, then the noise will depend of both b_{AB} (which represents the dimension of burts in the input) and r . The case when r is small is the more interesting one, because it is where the reverse transport is slow, which is common in natural active transport mechanisms. In such a situation, input noise is always reduced to a Fano factor smaller than $\frac{1+b_{AB}}{4}$, requiring $b_{AB} \geq 4$ to exceed Poisson noise in the output. In Figure 2 we plot the upper bound of F_{A_2} and F_{B_2} as a function of r and b_{AB} with the further assumption that $k_A = k_B$. As expected, when $b_{AB} = 1$, the noise is always half of Poisson (Fano factor of $\frac{1}{2}$), instead for $b_{AB} > 1$, the noise reduction depends on r , and always converges to half of Poisson for $r \rightarrow \infty$. Thus, preference towards the reverse direction of the symporter will always reduce noise to half of Poisson, while facilitated diffusion ($r=1$) and active transport against the gradient can also lead to such reduction, in case the input noise is limited.

Antiporters co-transport different molecule types in the opposite direction, picking up them at the two separate sides of the membrane and after a flip releasing on the other side. This can be modelled by the transport of molecules A and B between compartments 1 and 2 with the following reactions (Figure 1.III.)



Although the mechanism is different, at this level of description the reactions in (8) are identical to the ones

in (5). Hence, under the same assumptions, the same analysis applies to this system, resulting in

$$\frac{1}{2} \leq F_{A_2} \leq \frac{k_A + b_{AB}k_A + 4\sqrt{k_A k_B r} + k_B + b_{AB}k_B}{4(k_A + 2\sqrt{k_A k_B r} + k_B)} \quad (9)$$

and similarly for F_{B_2} , where $b_{AB} = b_A = b_B$.

Including Degradation in the Model

In the previous analysis we implicitly assumed that the transport is much faster than any degradation, so that internal loss of molecules can be neglected. Although this is a reasonable assumption for many natural systems, the degradation of the species will influence the noise in the limit. Hence, it is important to explicitly include species degradation in the model in order to get a clear picture of the noise reduction capabilities of the mechanisms presented in the previous sections. Therefore, in what follows, we extend the symporter model in Figure 1.II by assuming that species A and B are degraded with the same rate d both in compartment 1 and 2. Then, under the assumption that A and B appear in compartment 1 with Poisson processes with same mean $\frac{k_A}{k_{dA}}$, we obtain

$$F_{A_2} = F_{B_2} \approx \frac{3}{4}$$

$$F_{A_1} = F_{B_1} \approx 1 + \frac{\sqrt{k_A^2 r d^2}}{4r k_A (d + k_{dA})},$$

which hold under the assumption that the transport rate is faster than all the other rates, as common in natural systems. Note that the Fano factor of A_2 and B_2 is always smaller than 1 (Poisson noise) for any combination of the parameters. However, if one considers the Fano factor of A_1 or B_1 at steady state, this is always greater than 1. Hence, this suggests that the symporter mechanism reduces the noise in one compartment by increasing the noise in the compartment where the species are produced. This is an important observation, because it implies that when a molecule is transported inside the cell from the external environment through a symporter membrane protein, then the molecules inside the cell will be less noisy than outside.

Note that, being symporters and antiporters symmetric, what we discussed in this section also holds for antiporters.

COUPLED TRANSPORTERS

Transporters work in combination with primary transporters such as the Na-K-ATPase antiporter establishing opposing gradients of sodium and potassium, through the expenditure of ATP. These gradients are then used as an energy source by secondary transporters to ferry other

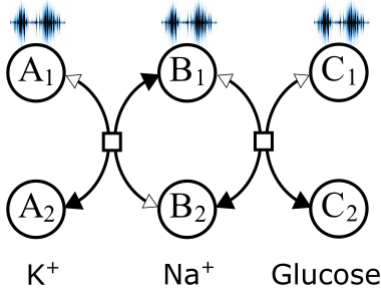
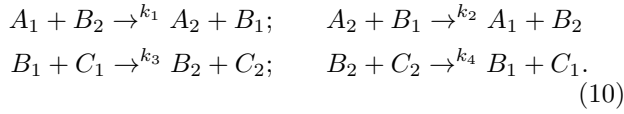


FIG. 3. Combination of an antiporter with a symporter. In this example we consider a sodium-potassium antiporter pump coupled with a glucose-sodium symporter [18]. We test with this how extracellular (top, molecules with subscript 1) noise in all three molecules could affect intracellular (bottom, molecules with subscript 2) signals downstream of these molecules.

ions and molecules across the cell membrane. A simple interaction between primary and secondary transporters is depicted in (Figure 5) where an antiporter (left) establishes a gradient in the B molecules that can be used by a symporter (right) to ferry C molecules inside the cell, and the relative reactions are modelled here below. We assume a noisy environment outside the cell (top) and we investigate the corresponding noise levels inside the cell (bottom).



In order to derive simple enough analytic expressions, we need to introduce some assumptions. First, we assume all species outside the cell are affected by Poisson noise with expected value respectively of p_A, p_B, p_C . Moreover, we fix the rates $k_1 = 2$ and $k_2 = 0.1$, whose ratio is taken from plausible biological conditions, assuming a fast export of sodium coupled to fast import of potassium [18]. Finally, we further assume $k_3 = k_4 = k$ meaning that the symporter works without a preferred direction and only uses the earlier established gradient of sodium to bring glucose into the cells. Under these assumptions we can obtain expressions for the Fano factors of the various species at steady state:

$$F_{A_2} = \frac{p_B + 10p_C}{p_B + 20p_C} \quad F_{B_2} = \frac{p_B + 40p_C}{2(p_B + 20p_C)} \quad F_{C_2} = \frac{1}{2}$$

Interestingly, as in Eqn (7) and Eqn (9), the Fano Factor of the intracellular C species is always $\frac{1}{2}$, independently of the reaction rates and the molecular levels of A, B, C outside the cell. This shows how the results obtained when studying symporters and antiporters in isolation can still hold for more complex architectures. For A and B, instead, the Fano factors depend on the molecular levels of the various species outside the cell. For A_2 , the noise is always sub-Poisson.

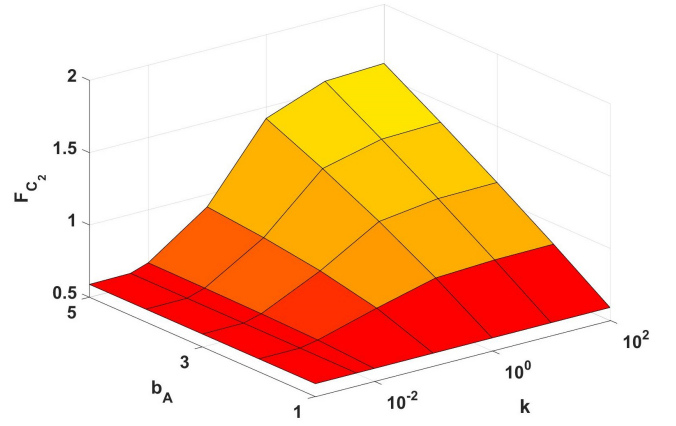


FIG. 4. Fano Factor intracellular glucose. The Figure plots the Fano factor of C_2 at steady state as a function of the rate of the transport $k = k_3 = k_4$ and the bursts on the input process b_A . The figure has been obtained numerically by solving the LNA.

Beyond these analytic results, we can remove some of the simplifying assumptions by performing numerical simulations. In Figure 5 we consider a more biologically realistic model (see Figure 8 in the Supplementary Material for a full description of the biological process), where we consider super Poisson noise outside the cell, a weaker reverse reaction for the symporter, and a stoichiometry for the antiporter matching a sodium-potassium pump [21]. That is, we replace the first two reactions in (10) with



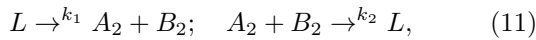
We next use the Linear Noise Approximation (LNA) [3, 5, 19] to numerically estimate the Fano factors. In Figure 4 we plot the resulting Fano factor for the intracellular C species. It is possible to observe that, consistently with the analytic results, we still have that when $b_A = 1$ (Poisson noise outside the cell), then F_{C_2} is independent of k and ≈ 0.6 . However, when $b_A > 1$ then this system can still reduce the noise for any value of k . Nevertheless, the smaller the k the more noise is filtered out.

DISCUSSION

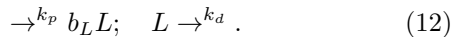
Various network motifs, such as feedback and feed-forward loops and annihilation filters, have been shown to reduce the noise in a homogeneous environment and the vast majority of related works focused on studying the noise suppression capabilities of these systems (see e.g., [11, 12, 14]). In contrast, in this paper we show that spatial compartmentalization, and active mechanisms of transport in particular, are themselves efficient noise reduction mechanisms often leading to sub-Poisson variability. Due to the ubiquitous nature of spatial compartmentalization in eukaryotic cells, this suggests that phys-

ical compartmentalization can be the dominant mechanism of noise reduction in eukaryotes. Network motifs can still be employed to further reduce the noise when particular precision is required. In fact, although symporters and antiporters naturally lead to sub-Poisson variability, these cannot reduce the noise to 0, which instead can be achieved with certain non-linear network motifs [11].

A key question is: what features of symporters and antiporters are responsible for their effective noise reducing capabilities? To investigate this issue we have tested sub-networks and found that the reversible release reaction of symporters and antiporters is an effective noise reducing network motif in itself. For instance, if we consider a simple decomplexation situation given by the following reactions, where a complex L , reversibly releases his components, A_2 and B_2 , at a given rate



where we assume that L noise is modelled, for $b_L > 0$, by



Then, we can show that for any value of k_1 it holds that:

$$\frac{1}{2} \leq F_{A_2} = F_{B_2} \leq \frac{(1 + b_L)\sqrt{k_d} + 4\sqrt{b_L r k_p}}{4(\sqrt{k_d} + 2\sqrt{r b_L k_p})}.$$

where $k_2 = k_1 \cdot r$, for $r \in \mathbb{R}_{>0}$. This implies that for $b_L = 1$ (Poisson input noise) we again have $F_{A_2} = F_{B_2} = \frac{1}{2}$ (half of Poisson independently of the rates). A similar pattern also occurs in the annihilation module proposed in [11] and a similar motif including a self-cleavage ribozyme has been shown to improve translational efficiency in [4]. Thus, this suggests that a simple network motif combining complex formation and release steps may be a general motif for noise reduction.

In a biological example we have also focused on a system where a sodium - potassium antiporter pump creates a gradient of sodium that facilitates glucose import through a sodium - glucose symporter. Similar systems have been modelled by others [18], but here we show that this system can reduce the intracellular noise on glucose levels. Certainly this is just a small part of the glucose transport system as glucose can be imported in other ways [20] and it is also rather quickly processed into glucose 6-phosphate. Still, the mechanism proposed here could serve as a noise reducing module ensuring that intracellular glucose signalling pathways are robustly controlled and do not give false signals for noise.

ACKNOWLEDGMENTS

L.C. is funded by a Royal Society Professorship.

-
- [1] Battich, N., Stoeger, T., and Pelkmans, L., *Cell* **163**, 1596 (2015).
- [2] Becskei, A. and Serrano, L., *Nature* **405**, 590 (2000).
- [3] Cardelli, L., Kwiatkowska, M., and Laurenti, L., *Biosystems* **149**, 26 (2016).
- [4] Delalez, N., Sootla, A., Wadhams, G. H., and Papatristodoulou, A., *BioRxiv*, 504449 (2018).
- [5] Grima, R., *Physical Review E* **92**, 042124 (2015).
- [6] Hansen, M. M., Desai, R. V., Simpson, M. L., and Weinberger, L. S., *Cell systems* **7**, 384 (2018).
- [7] Hilfinger, A., Norman, T. M., Vinnicombe, G., and Paulsson, J., *Physical review letters* **116**, 058101 (2016).
- [8] Kaern, M., Elston, T. C., Blake, W. J., and Collins, J. J., *Nature Reviews Genetics* **6**, 451 (2005).
- [9] Kaiser, C. A., Krieger, M., Lodish, H., and Berk, A., *Molecular cell biology*. (WH Freeman, 2007).
- [10] Kitano, H., *Nature Reviews Genetics* **5**, 826 (2004).
- [11] Laurenti, L., Csikasz-Nagy, A., Kwiatkowska, M., and Cardelli, L., *Biophysical Journal* **114**, 3000 (2018).
- [12] Lestas, I., Vinnicombe, G., and Paulsson, J., *Nature* **467**, 174 (2010).
- [13] Samoilov, M., Arkin, A., and Ross, J., *The Journal of Physical Chemistry A* **106**, 10205 (2002).
- [14] Schmiedel, J. M., Klemm, S. L., Zheng, Y., Sahay, A., Blüthgen, N., Marks, D. S., and van Oudenaarden, A., *Science* **348**, 128 (2015).
- [15] Singh, A. and Bokes, P., *Biophysical journal* **103**, 1087 (2012).
- [16] Smith, S. and Grima, R., *Nature Communications* **9**, 345 (2018).
- [17] Stoeger, T., Battich, N., and Pelkmans, L., *Cell* **164**, 1151 (2016).
- [18] Thorsen, K., Drensting, T., and Ruoff, P., *American Journal of Physiology-Cell Physiology* **307**, C320 (2014).
- [19] Van Kampen, N. G., *Stochastic processes in physics and chemistry*, Vol. 1 (Elsevier, 1992).
- [20] Wood, I. S. and Trayhurn, P., *British journal of nutrition* **89**, 3 (2003).
- [21] Wright, E. M., Loo, D. D., and Hirayama, B. A., *Physiological reviews* **91**, 733 (2011).

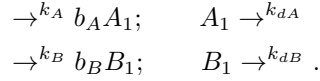
SUPPLEMENTARY MATERIAL

In Section "Mathematical Details for Symporter and Antiporter Mechanisms" we provide the derivation of the Fano factor expressions for symporters and antiporters in the main text, including the case when the degradation of the species is explicitly included in the model. In Section "Why Symporters and Antiporters Reduce Noise" we discuss the reasons why these systems filter noise. Then, in Section "Alternative Models" we present variations of symporter and antiporter models and discuss their noise reduction capabilities. In Section "Mathematical Details for the Uniporter Mechanism" we provide the derivation of the mathematical expressions for the uniporter system reported in the main text, Finally, in Section "Numerical Analysis" we perform numerical analysis to validate our results with stochastic simulations and numerical solutions of the Chemical Master Equation (CME).

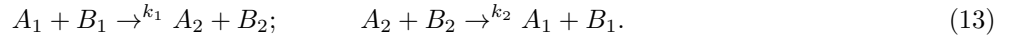
MATHEMATICAL DETAILS OF SYMPORTER AND ANTIPORTER MECHANISM

As symporters and antiporters mechanisms are equivalent, we only give details for symporter transports.

We first assume that molecules of species A and B appear in compartment 1 by a noisy process modelled by the following reactions. This may model noisy extra-cellular transport of molecules in compartment 1



A and B molecules are transported from compartment 1 to compartment 2 and vice-versa according to the following reactions



To study the covariance matrix of the system at steady state we can consider the Lyapunov matrixial equation [3]

$$J_F C + C J_F^T + W = 0, \quad (14)$$

where for $v_1 = \begin{bmatrix} 1 \\ 0 \\ 0 \\ 0 \end{bmatrix}$, $v_2 = \begin{bmatrix} -1 \\ 0 \\ 0 \\ 0 \end{bmatrix}$, $v_3 = \begin{bmatrix} 0 \\ 0 \\ 1 \\ 0 \end{bmatrix}$, $v_4 = \begin{bmatrix} 0 \\ 0 \\ -1 \\ 0 \end{bmatrix}$, $v_5 = \begin{bmatrix} -1 \\ 1 \\ -1 \\ 1 \end{bmatrix}$, $v_6 = \begin{bmatrix} 1 \\ -1 \\ 1 \\ -1 \end{bmatrix}$, we have that W is the diffusion matrix such that

$$\begin{aligned} W = & v_1 v_1^T k_A + v_2 v_2^T k_{dA} E[A_1]_\infty \\ & + v_3 v_3^T k_B + v_4 v_4^T k_{dB} E[B_1]_\infty \\ & + v_5 v_5^T k_1 E[A_1]_\infty E[B_1]_\infty + v_6 v_6^T k_2 E[A_2]_\infty E[B_2]_\infty, \end{aligned}$$

with $E[A_i]_\infty, E[B_i]_\infty$ being the expectation of A_i and B_i at steady state. J_F is the Jacobian of vector

$$\begin{aligned} F = & v_1 k_A + v_2 k_{dA} E[A_1]_\infty \\ & + v_3 k_B + v_4 k_{dB} E[B_1]_\infty \\ & + v_5 k_1 E[A_1]_\infty E[B_1]_\infty + v_6 k_2 E[A_2]_\infty E[B_2]_\infty, \end{aligned}$$

with respect to the different species and

$$C = \begin{bmatrix} C[A_1]_\infty & C[A_1 A_2]_\infty & C[A_1 B_1]_\infty & C[A_1 B_2]_\infty \\ C[A_1 A_2]_\infty & C[A_2]_\infty & C[A_2 B_1]_\infty & C[A_2 B_2]_\infty \\ C[A_1 B_1]_\infty & C[A_2 B_1]_\infty & C[B_1]_\infty & C[B_1 B_2]_\infty \\ C[A_1 B_2]_\infty & C[A_2 B_2]_\infty & C[B_1 B_2]_\infty & C[B_2]_\infty \end{bmatrix}$$

is the covariance matrix of the system. Note that Eqn (14), although exact for linear reaction systems (those not containing multi-molecular reactions), is only an approximation for general non-linear reaction networks. Nevertheless, for non-linear models the exact expression of the variance of the various species in general cannot be obtained, as it would require the solution of a system of a non-finite number of equations (the so-called moment closure problem). Hence, Eqn (14) is often employed and has been shown to be a surprisingly good approximation also for non-linear

systems [3, 19]. Moreover, our analytic expressions are validated through numerical analysis in Section Numerical Analysis.

As Eqn (14) admits infinitely many solutions, we need a further constraint that depends on the initial conditions. By writing (14) it is possible to realize that, assuming that the species are known at time 0 (variances and covariances are all 0 at the initial time), we have that the following equation holds

$$C[A_2 B_2]_\infty = C[A_2]_\infty$$

. That is, the covariance between A_2 and B_2 is equal to the variance of A_2 (or equivalently of B_2) at steady state.

Exact expression of F_{B_2} and F_{A_2} can be obtained by solving the resulting system of equations, which has only one admissible solution. This can be done using an appropriate tool for symbolic calculation (we used Mathematica). However, the resulting expression will be very complex. Hence, for the sake of obtaining simpler analytic solutions, we assume $k_{dA} = k_{dB}$ and $b_A = b_B$. That is, the two inputs (A_1 and B_1) are produced by processes with same Fano factor (see Eqn (3) in the main text), but possibly different expected value. Moreover, we consider $k_1 = r$ and $k_2 = k \cdot r$. We obtain

$$F_{A_2} = F_{B_2} = \frac{2k_{dA}^4 + 3k_{dA}^2 b_{AB} k k_A + k_{dA}^2 b_{AB}^2 k k_A + b_{AB}^2 k^2 k_A^2 + b_{AB}^3 k^2 k_A^2 + 2\sqrt{r} b_{AB}^2 k^2 k_A^{\frac{3}{2}} \sqrt{k_B} - 2\sqrt{r} b_{AB}^3 k^2 k_A^{\frac{3}{2}} \sqrt{k_B}}{4(k_{dB}^4 + 2k_{dB}^2 b_{AB} k k_A + b_{AB}^2 k^2 k_A^2 + 2k_{dB}^2 b_{AB} k k_B + 2b_{AB}^2 k^2 k_A k_B - 4r b_{AB}^2 k^2 k_A k_B + b_{AB}^2 k^2 k_B^2)} \\ + \frac{+3k_{dA}^2 b_{AB} k k_B k_{dA}^2 b_{AB}^2 k k_B + 2b_{AB}^2 k^2 k_A k_B - 8r b_{AB}^2 k^2 k_A k_B + 2b_{AB}^3 k^2 k_A k_B + 2\sqrt{r} b_{AB}^2 k^2 \sqrt{k_A} k_B^{\frac{3}{2}}}{4(k_{dB}^4 + 2k_{dB}^2 b_{AB} k k_A + b_{AB}^2 k^2 k_A^2 + 2k_{dB}^2 b_{AB} k k_B + 2b_{AB}^2 k^2 k_A k_B - 4r b_{AB}^2 k^2 k_A k_B + b_{AB}^2 k^2 k_B^2)} \\ - \frac{2\sqrt{k} b_{AB}^3 k^2 \sqrt{k_A} k_B^{\frac{3}{2}} + b_{AB}^2 k^2 k_B^2 + b_{AB}^3 k^2 k_B^2}{4(k_{dB}^4 + 2k_{dB}^2 b_{AB} k k_A + b_{AB}^2 k^2 k_A^2 + 2k_{dB}^2 b_{AB} k k_B + 2b_{AB}^2 k^2 k_A k_B - 4r b_{AB}^2 k^2 k_A k_B + b_{AB}^2 k^2 k_B^2)}$$

The above expression, although exact, does not offer many intuitions. Hence, we can study what happens in the limit of a very slow and very fast transport. We obtain

$$\lim_{k \rightarrow 0} F_{A_2} = \lim_{k \rightarrow 0} F_{B_2} = \frac{1}{2}.$$

Thus, no matter how noisy is the inputs production, in the limit of slow transport the resulting Fano Factor will always be $\frac{1}{2}$. Instead, for a fast transport we obtain

$$\lim_{k \rightarrow \infty} F_{A_2} = \lim_{k \rightarrow \infty} F_{B_2} = \frac{k_A + b_{AB} k_A + 4\sqrt{k_A k_B r} + k_B + b_{AB} k_B}{4(k_A + 2\sqrt{k_A k_B r} + k_B)}.$$

Now, in order to study what happens for any other value of k , we can study the derivative of F_{A_2} with respect to k . We obtain that for any fixed $b_A > 0, k_A > 0, k > 0, k_{dA} > 0$ the derivative of F_{A_2} with respect to k is always non-negative. Thus, we can conclude

$$\frac{1}{2} \leq F_{A_2} \leq \frac{k_A + b_{AB} k_A + 4\sqrt{k_A k_B r} + k_B + b_{AB} k_B}{4(k_A + 2\sqrt{k_A k_B r} + k_B)},$$

and similarly for F_{B_2} .

Instead, for deriving the mean of the various species at steady state, which are also needed to obtain a solution to Eqn (14), we can simply solve the system of polynomial equations

$$F = 0.$$

This corresponds to solve the well known rate equations at steady state [3].

Model of Symporter with Explicit Degradation of the Species

In the CRN (17) we implicitly assumed that the degradation of the species is much slower than the transport. Hence, any loss of molecules can be omitted from the model. This is not always the case. Therefore, in what follows we extend CRN (17) with the following reactions



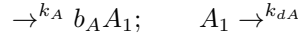
That is, all species are degraded at same rate d . We further assume $b_A = 1$ (i.e., Poisson input noise) and $k_A = k_B$ (i.e., $E[A_1]_\infty = E[B_1]_\infty$). Then, with the techniques derived in the previous section, we can derive analytic expressions for $F_{A_1}, F_{A_2}, F_{B_1}, F_{B_2}$. Moreover, if we link k_1 and k_2 such that $k_2 = k_1 r$ we obtain

$$\begin{aligned}\lim_{k_1 \rightarrow \infty} F_{A_1} &= \lim_{k_1 \rightarrow \infty} F_{B_1} = 1 + \frac{\sqrt{k_A^2 r d^2}}{4 r k_A (d + k_{dA})} \\ \lim_{k_1 \rightarrow \infty} F_{A_2} &= \lim_{k_1 \rightarrow \infty} F_{B_2} = \frac{3}{4}\end{aligned}$$

WHY SYMPORTERS AND ANTIPORTERS REDUCE NOISE?

Complex Release Model

In this Section we consider an input species A_1 arriving with a noise process modelled by the following reactions



with $b_A \in \mathbb{Z}_{\geq 0}$. We consider the following mechanism



That is, we have a complex A_1 which is produced by a noisy process. The complex may spontaneously change configuration (A_2) and release a product B_2 . We are interested in studying the noise properties for A_2 and B_2 . To do that we can use the Lyapunov Eqn (14) to derive an analytic form for the variance of A_2 and B_2 a steady state. In order to obtain a unique solution, as A_2 and B_2 are always produced and consumed together, we can assume

$$C[A_2 A_2]_\infty = C[B_2 B_2]_\infty \quad C[A_2 B_2]_\infty = C[B_2 B_2]_\infty.$$

Under these assumptions we have that the Fano factor of A_2 and B_2 is given by

$$F_{A_2} = F_{B_2} = \frac{(1 + b_L)k\sqrt{k_d} + 4k\sqrt{b_L r k_p} + 2k_d\sqrt{k_d}}{4(\sqrt{k_d}(k + k_d) + 2k\sqrt{r b_L k_p})}, \quad (15)$$

where in the above expression we have assumed $k_1 = k$ and $k_2 = r \cdot k$. Now we can study what happens in the limit of infinitely slow and fast transport, and we have

$$\begin{aligned}\lim_{k \rightarrow 0} F_{A_2} &= \lim_{k \rightarrow 0} F_{B_2} = \frac{1}{2} \\ \lim_{k \rightarrow \infty} F_{A_2} &= \lim_{k \rightarrow \infty} F_{B_2} = \frac{(1 + b_L)\sqrt{k_d} + 4\sqrt{b_L r k_p}}{4(\sqrt{k_d} + 2\sqrt{r b_L k_p})}\end{aligned}$$

Note that this implies that if $b_A = 1$ (Poisson noise) then $F_{A_2} = F_{B_2} = \frac{1}{2}$ no matter the other parameter values.

If we now take the partial derivative of F_{A_2} with respect to k , we obtain this is always non-negative. Hence, we can conclude that for fixed and finite parameters, we obtain

$$\frac{1}{2} \leq F_{A_2} = F_{B_2} \leq \frac{(1 + b_L)\sqrt{k_d} + 4\sqrt{b_L r k_p}}{4(\sqrt{k_d} + 2\sqrt{r b_L k_p})}.$$

ALTERNATIVE SYMPORTER MODELS

Molecular symporters and antiporters, such as the sodium-potassium pump or the Na-K-Cl cotransporter are of course much more complex than the simple reactions in (5). Those system fundamentally transfer molecules between compartments, but they do so through a number of intermediate stages, by first collecting all the input molecules, then triggering conformational changes, and finally releasing the output molecules, all the while consuming and producing additional substances. It is not obvious that the noise reduction observed for Equation (5) would carry over to these systems. However, the noise reduction appears to be intrinsic to the input-output behavior of the systems, rather than

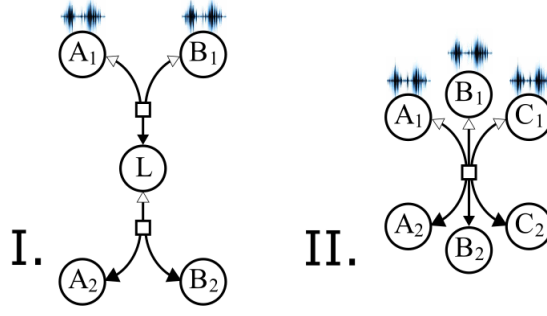
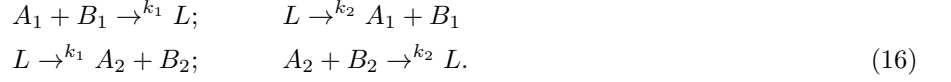


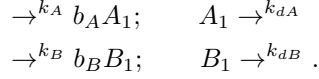
FIG. 5. Extended Symporters.

to their detailed internal structure. Simulations, however, do not offer a precise explanation for this phenomenon. To investigate this issue further we now study, analytically, a model of intermediate complexity, where there is one intermediate stage during the transport, summarizing all the intermediate conformational changes that are present in actual transporters (Figure 8). The consistent behavior of simulations for detailed models, with the analytic solutions of increasingly simplified models, will then suggest a plausible explanation for the behavior of the biochemical systems.

We consider the following extended model of the symporter



We assume that A and B appears in compartment 1 through a noisy process modelled by the following reactions



For simplicity we assume that $b_A = b_B$, $k_A = k_B$, and $k_{dA} = k_{dB}$. Then, we have

$$\frac{1}{2} \leq F_{A_2} = F_{B_2} \leq \frac{4b_A k_A + k_{dA} + b_A k_{dA} + 2k_{dA} r}{8b_A k_A + 4k_{dA} + 4k_{dA} r},$$

where in the above equations, we assumed

$$k_1 = k; \quad k_2 = k \cdot r.$$

More precisely, we obtain

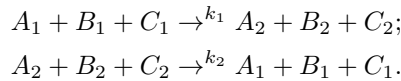
$$\lim_{k \rightarrow 0} F_{A_2} = \lim_{k \rightarrow 0} F_{B_2} = \frac{1}{2},$$

$$\lim_{k \rightarrow \infty} F_{A_2} = \lim_{k \rightarrow \infty} F_{B_2} = \frac{4b_A k_A + k_{dA} + b_A k_{dA} + 2k_{dA} r}{8b_A k_A + 4k_{dA} + 4k_{dA} r},$$

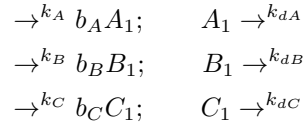
with the Fano Factor increasing monotonically with k . Note that this again implies that if $b_A = 1$ then $F_{A_2} = F_{B_2} = \frac{1}{2}$ independently of the rates of the symporter. Hence, this confirms that the results obtained for the simplified symporters and antiporters in the main text, still hold for more complex models.

Symporter Trimolecular

Certain molecular transporters transfer more than two molecules at once. Hence, we consider the following extended model of symporter



We assume that A, B and C appear in compartment 1 through extra-cellular transport with a noisy mechanism modelled by the following reaction



For simplicity we assume that $b_A = b_B = b_C$, $k_A = k_B = k_C$, and $k_{dA} = k_{dB} = k_{dC}$. Then, we have

$$\frac{1}{3} \leq F_{A_2} = F_{B_2} = F_{C_2} \leq \frac{1 + b_A + 2r^{\frac{1}{3}}}{6 + 6r^{\frac{1}{3}}},$$

where in the above equations we assumed

$$k_1 = k; \quad k_2 = k \cdot r.$$

More precisely, we obtain

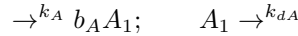
$$\lim_{k \rightarrow 0} F_{A_2} = \lim_{k \rightarrow 0} F_{B_2} = \lim_{k \rightarrow 0} F_{C_2} = \frac{1}{3},$$

$$\lim_{k \rightarrow \infty} F_{A_2} = \lim_{k \rightarrow \infty} F_{B_2} = \lim_{k \rightarrow \infty} F_{C_2} = \frac{1 + b_A + 2r^{\frac{1}{3}}}{6 + 6r^{\frac{1}{3}}},$$

with the Fano Factor increasing monotonically with k . Note that this implies that if $b_A = 1$ then $F_{A_2} = F_{B_2} = \frac{1}{3}$ independently of the rates of the symporter. The improved noise reduction capabilities are due to the tri-molecular reactions. In fact, if we model this system as a sequence of bi-molecular reactions, we recover the lower bound of $\frac{1}{2}$ reported in the main text.

MATHEMATICAL DETAILS FOR UNIORTER MECHANISM

We again assume that molecules of species A appear in compartment 1 through a noisy process modelled by the following reactions



and are transported from compartment 1 to compartment 2 and vice-versa according to the following reactions



To study the covariance matrix of the system at steady state we notice that the reaction network considered in this Section is composed only by uni-molecular reactions. Hence, if we consider the Lyapunov matrixial equation in Eqn (14) and the rate equations, their solution gives the exact variance and mean of the species [5]. In particular, at steady state, we obtain the following system of equations.

$$\begin{aligned} E[A_2]_{\infty} k_2 - E[A_1]_{\infty} k_1 - E[A_1]_{\infty} k_{dA} + b_A k_A &= 0 \\ E[A_1]_{\infty} k_1 - E[A_2]_{\infty} k_2 &= 0 \\ k_A b_A^2 + E[A_1]_{\infty} k_1 + E[A_2]_{\infty} k_2 + E[A_1]_{\infty} k_{dA} + 2 * C[A_1 A_2]_{\infty} k_2 - 2 * C[A_1]_{\infty} (k_1 + k_{dA}) &= 0 \\ C[A_1]_{\infty} k_1 - E[A_2]_{\infty} k_2 - E[A_1]_{\infty} k_1 - C[A_1 A_2]_{\infty} k_2 + C[A_2]_{\infty} k_2 - C[A_1 A_2]_{\infty} (k_1 + k_{dA}) &= 0 \\ E[A_1]_{\infty} k_1 + E[A_2]_{\infty} k_2 + 2C[A_1 A_2]_{\infty} k_1 - 2C[A_2]_{\infty} k_2 &= 0 \end{aligned}$$

The system has a unique solution characterized by the following variance and mean for A_2 at steady state

$$\begin{aligned} E[A_2]_{\infty} &= \frac{k_1}{k_2} E[A_1]_{\infty} = \frac{k_1 b_A k_A}{k_2 k_{dA}} \\ C[A_2]_{\infty} &= \frac{b_A k_1 k_A (k_1 + b_A k_1 + 2k_2 + 2k_{dA})}{2k_2 k_{dA} (k_1 + k_2 + k_{dA})}. \end{aligned}$$

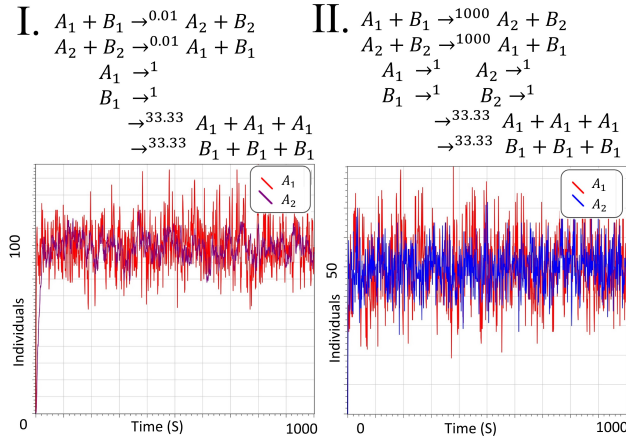


FIG. 6. Comparison of a model where the degradation of the species is assumed to be slower compared to all the other rates (I) and one where degradation of the species is explicitly considered (II). All plots are obtained by performing stochastic simulations of the Chemical Master Equation (CME) [19]. In both cases it is possible to observe how A_2 has reduced variability.

NUMERICAL ANALYSIS

Although Eqn (14) is exact for linear systems, for general non-linear reaction networks it is only an approximation. Hence, in what follows we validate our results with simulations of the Chemical Master Equation (CME) [19].

In Figure 6 we perform stochastic simulations of a symporter that transports molecules A and B from compartment 1 to compartment 2. In Figure 6.I we consider a model where A_1 and B_1 have super-Poisson noise. Same input processes are considered also for 6.II, but we also include the degradation of the species in the model and consider a faster transport. As expected, in both cases, A_2 and B_2 have reduced variability compared to the input species.

In Figure 7 we again consider a symporter transport with super-Poisson noise on the first compartment and we numerically estimate the time evolution of mean and variance. In Figure 7.I we consider the approximations we employed to derive analytic expression of the Fano factors in the main text. Then, in Figure 7 we numerically solve the CME. In both cases the symporter reduces the variance of the species in the compartment where they are not produced.

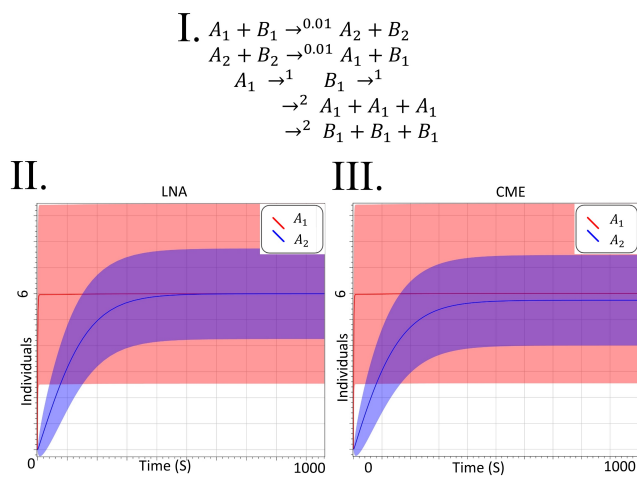


FIG. 7. We consider a reaction network where a symporter is used to transport molecules of species A and B between two compartments (I). In II we plot the time evolution of mean and variance A_1 and A_2 according to the Linear Noise Approximation (LNA). That is, the mean is estimated by solving the rate equations and the variance is estimated by solving the system of ODEs associated to Eqn (14). In III we plot the time evolution of the same species according to the Chemical Master Equation (CME). It is possible to observe that while the variance predicted by Eqn (14) is very similar to that obtained by the CME, the mean is slightly different. This is due to the fact that the mean is estimated according to the rate equations, which neglect corrections terms of order higher than the first to estimate the mean. Note that this difference becomes less and less important the more molecules are in the system and is already negligible when A_1 and B_1 have a mean of few tens of molecules at steady state.

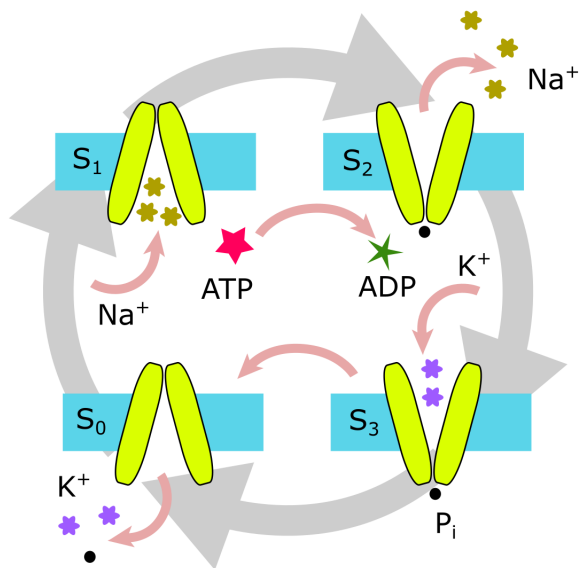


FIG. 8. The sodium-potassium pump cycle.